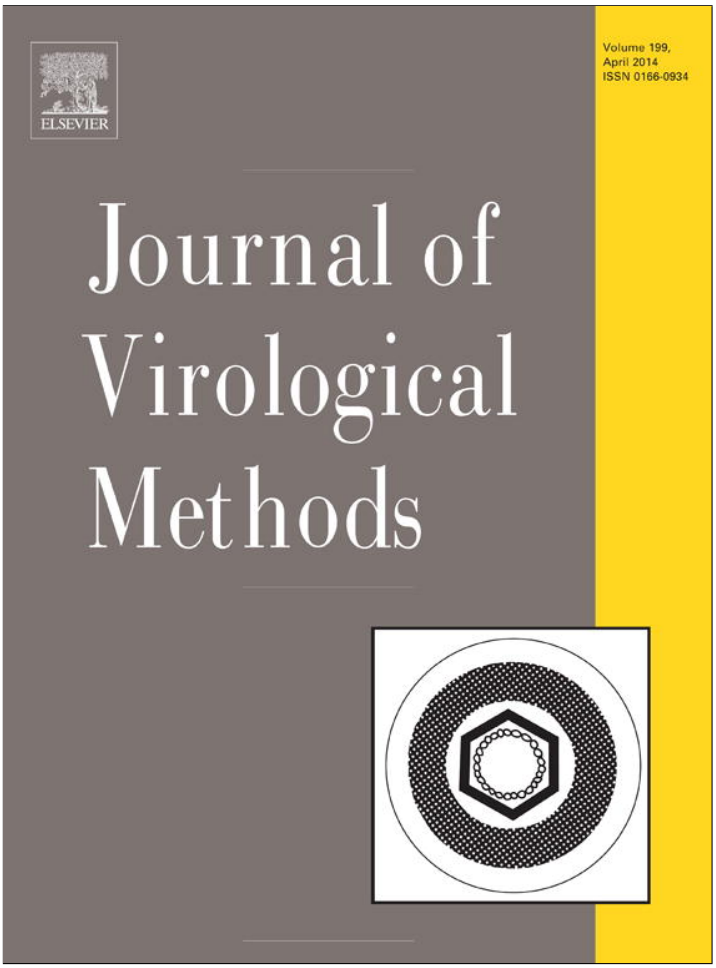

Journal of Virological Methods 199 (2014) 1–10

Contents lists available at ScienceDirect

Journal of Virological Methods

journal homepage: www.elsevier.com/locate/jviromet

Artificial microRNAs as antiviral strategy to FMDV: structural implications of target selection

María Inés Gismondi, Xoana P. Ortiz, Anabella P. Currá, Sebastián Asurmendi*, Oscar Taboga

Instituto de Biotecnología, CICVyA, INTA, Dr. N. Repetto y Los Reseros s/n, CP 1686 Hurlingham, Buenos Aires, Argentina

Article history:
Received 18 July 2013
Received in revised form
10 December 2013
Accepted 17 December 2013
Available online 7 January 2014

Keywords:
Artificial microRNAs
Antiviral
FMDV
Accessibility
RNA structure

A B S T R A C T

RNA interference (RNAi) appears as a promising strategy to control virus replication. While the antiviral power of short-hairpin RNAs or small-interfering RNAs against FMDV has been demonstrated widely, safer RNAi effectors such as artificial microRNAs (amiRs) have not been evaluated extensively. In this work, transgenic monoclonal cell lines constitutively expressing different amiRs targeting FMDV 3D-coding region or 3′UTR were established. Certain cell lines showed an effective, sequence-specific amiR-mediated silencing activity that was accomplished by degradation of the target mRNA, as demonstrated in co-transfection experiments of reporter genes fused to FMDV target sequences. However, FMDV replication in these amiR-expressing cells was affected barely. Experiments aimed at elucidating the cause of RNAi failure demonstrated limited accessibility of the targeted region in the molecular environment of the viral RNA. Since RNAi is mediated by large-dimension silencing complexes containing the siRNA and not simply by a linear oligonucleotide, we propose that target selection should consider not only the local RNA structure but also the global conformation of target RNA.

1. Introduction

Foot-and-mouth disease (FMD) is a highly contagious viral disease of major socioeconomic importance affecting domestic and wild cloven-hoofed animals (Grubman and Baxt, 2004). The etiological agent, FMD virus (FMDV, member of the genus *Aphthovirus* in the *Picornaviridae* family), consists of a single-stranded positive-sense RNA molecule surrounded by an icosahedral capsid composed of four viral proteins (Rueckert, 1996). The viral genome is approximately 8500 nucleotides long and encodes a polyprotein precursor that is cleaved post-translationally to originate the mature viral proteins including the RNA-dependent RNA polymerase (3D), a highly conserved enzyme that catalyzes viral RNA replication (Carrillo et al., 2005). At both its 5′ and 3′ ends, the FMDV RNA contains highly structured untranslated regions (UTRs) relevant for the viral replication cycle. Additionally, the genomic RNA is covalently linked to a viral polypeptide (VPg) at its 5′ end and contains a genetically coded poly(A) tail at its 3′ terminus (Grubman and Baxt, 2004).

The virus is antigenically highly variable, and there are seven serotypes (A, C, O, Asia, SAT1, SAT2 and SAT3) and multiple subtypes (Domingo et al., 2003). Current vaccines based on inactivated whole virus have been effective in controlling FMD from susceptible animal populations, albeit without efficient cross-protection across serotypes or subtypes. Furthermore, inactivated vaccines need ~7 days to induce immune protection, and so their use is limited in case of outbreaks particularly in disease-free countries. Consequently, there is a need to develop new antiviral tools that provide early protection or ideally block viral replication thereby restraining FMD spread.

RNA interference (RNAi) is a sequence-specific post-transcriptional gene silencing phenomenon triggered by double-stranded RNA and mediated by small RNAs (small interfering RNAs [siRNAs] or microRNAs [miRs], among others) that leads ultimately to degradation or translational repression of the targeted transcript. RNAi has been proposed as an alternative means to control virus replication including FMDV (Grubman and de los Santos, 2005; van Rij and Andino, 2006; Arbuthnot, 2011). In fact, the antiviral activity of RNAi against FMDV has been demonstrated widely both *in vitro* and *in vivo* using synthetic siRNAs as well as plasmid- or virus-encoded short hairpin RNAs (shRNAs) targeting different regions of the viral genome (Chen et al., 2004; Kahana et al., 2004; Liu et al., 2005; Chen et al.,

* Corresponding author at: Instituto de Biotecnología, CICVyA, INTA, Dr. N. Repetto y Los Reseros s/n, CP 1686 Hurlingham, Buenos Aires, Argentina.
Tel.: +54 11 4621 1447; fax: +54 11 4621 0199.
E-mail addresses: mgismondi@cnia.inta.gov.ar (M.I. Gismondi), xoanaortiz@hotmail.com (X.P. Ortiz), anabellapaola06@yahoo.com.ar (A.P. Currá), asurmendi.sebastian@inta.gob.ar, sasurmendi@cnia.inta.gov.ar (S. Asurmendi), otaboga@cnia.inta.gov.ar (O. Taboga).

0166-0934/$ – see front matter © 2013 Elsevier B.V. All rights reserved.
http://dx.doi.org/10.1016/j.jviromet.2013.12.016

2006; Kim et al., 2008, 2010). However, shRNAs may disrupt the endogenous miR pathway in transfected cells, so the use of plasmid-encoded artificial miRs has been favored (Boudreau et al., 2009). Indeed, the antiviral power of amiRs has been demonstrated (Son et al., 2008; Israsena et al., 2009; Du et al., 2011).

A major obstacle faced by RNAi technology for therapeutic use is the need of effective, safe and reliable delivery systems (Castanotto and Rossi, 2009). Given the rapid spread of FMD, RNAi-based antivirals should block ideally the first cycle of viral replication and thus limit disease dissemination. In this sense, recent studies aimed at the development of transgenic animals naturally resistant to FMDV are challenging (Pengyan et al., 2010; Wang et al., 2012).

In this work, we have investigated the silencing activity of transgenic cell lines constitutively expressing amiRs targeting essential regions of FMDV genome. Our results point out the critical role played by RNA accessibility that is often overlooked during the design of RNAi-based antiviral approaches.

2. Materials and methods

2.1. Cells, viruses and virus titration

Baby hamster kidney (BHK-21 clone 13) cells were obtained from the American Type Culture Collection and maintained in Dulbecco's modified Eagle's medium (DMEM) supplemented with 10% fetal bovine serum (FBS) at 37 °C with 5% CO_2. Transgenic $amiR_{FMDV}^+$ cell lines were grown in DMEM supplemented with 10% FBS and 7 μg/ml blasticidin S (Invitrogen, Carlsbad, USA). FMDV A/Arg/01 (prototype strain MC267 from Trenque Lauquen, Genbank accession number AY593786) was obtained from the National Institute for Animal Health (SENASA, Argentina) (García Núñez et al., 2010).

Virus titers were determined in BHK-21 cells by plaque assay (pfu/ml) or alternatively the 50% tissue culture infective dose ($TCID_{50}$) was calculated using the formula of Reed and Muench (Reed and Muench, 1938).

2.2. Plasmids

2.2.1. Pre-amiR encoding plasmids

Target sequences were predicted on the FMDV genome (serotype A, strain A/Arg/01) using the *siRNA target Finder* (Ambion). To take into account target site accessibility during the amiR selection procedure, the candidate target sites were mapped within the secondary structure of the full-length FMDV RNA predicted as indicated in Section 2.9. Target sites located at positions 6853–6873, 7945–7965 and 8154–8174 of the viral genome (designated 3D1, 3D2 and 3UTR, respectively) were predicted to be less structured as other candidates within the same portion of the genome and accordingly they were selected to design the corresponding amiRs. Targets showing polymorphic positions mainly outside the seed region among FMDV serotypes circulating in South America (Fig. 1A) were selected intentionally to study the impact of such differences on the silencing ability of transgenic cells. Mature amiR sequences were: $amiR_{3D1}$ 5′-UUUCGUGUCUCCUUUGUGUUU-3′, $amiR_{3D2}$ 5′-UCCUGCCACAGAGAUCAACUU-3′ and $amiR_{3UTR}$ 5′-AGGAAGCGGAGAAAGCUCUUU-3′. Target sequences showed no similarity with mammalian genes.

Complementary single-stranded DNA oligonucleotides encoding each pre-amiR (Table 1) were synthesized, annealed and cloned into pcDNA®6.2-GW/miR vector (BLOCK-iT Pol II miR RNAi expression vector kit, Invitrogen, Carlsbad, USA) following the manufacturer's instructions. The resulting plasmids were named pcDNA6.2/$amiR_{3D1}$, pcDNA6.2/$amiR_{3D2}$ and pcDNA6.2/$amiR_{3UTR}$.

2.2.2. Luciferase reporter plasmids

Reporter plasmids encoding the *Renilla* luciferase gene (RLuc) fused to FMDV fragments enclosing amiR target sequences from serotypes A (A/Arg/01) or O (O1 Campos, Genbank Accession number AJ320488.1) were constructed. The RLuc coding sequence was amplified by PCR using oligonucleotides RLfor and RLrev (Table 1) and plasmid pRNull (Promega, Madison, USA) DNA as template. The amplified product was digested with *Eco*RV and cloned at the *Dra*I site of pcDNA6.2®-GW/miR-neg, originating plasmid pcDNA6.2/RLuc/miR-neg. DNA fragments encompassing amiR target sequences were obtained by fill-in (3D1 and 3UTR) or PCR (3D2) reactions using the primers listed in Table 1. For fill-in reactions, oligonucleotides were annealed and double-stranded DNA was elongated with Klenow fragment of DNA polymerase (Promega, Madison, USA). Products were purified from a 20% polyacrilamide gel and cloned into pGemT-Easy vector (Promega, Madison, USA). The 3D2-encompassing fragment was amplified from cDNAs derived from strains A/Arg/01 and O1 Campos and cloned into pGemT-Easy vector (Promega, Madison, USA). Fragments containing each target sequence were subcloned between the *Bam*HI and *Xho*I sites of vector pcDNA6.2/RLuc/miR-neg. Control plasmid pcDNA6.2/RLuc lacking the miR expression cassette was obtained by enzymatic digestion of plasmid pcDNA6.2/RLuc/miR-neg with *Bam*HI and *Bgl*II, followed by re-ligation of compatible ends.

To assess *in vitro* accessibility of target sequences, the T7 RNA polymerase promoter was excised from plasmid pGemLuc (Promega, Madison, USA) and subcloned between *Nde*I and *Sac*I restriction sites located upstream of the RLuc coding sequence in selected pcDNA6.2/RLuc-derived plasmids.

To construct plasmid pcDNA6.2/FLuc, the firefly luciferase (FLuc) coding sequence was excised from plasmid pGemLuc (Promega, Madison, USA) with *Bam*HI and *Xho*I enzymes and subcloned into plasmid pcDNA6.2®-GW/miR-neg.

All recombinant vectors were confirmed by automated sequencing.

2.3. Establishment of transgenic cell lines

Pre-amiR encoding plasmids were transfected into 95% confluent BHK-21 cells using Lipofectamine (Invitrogen, Carlsbad, USA), according to manufacturer's instructions. Transfected cells were subcultured after 24 h in DMEM medium containing 10% FBS and 7 μg/ml blasticidin S (Invitrogen, Carlsbad, USA). Polyclonal cell lines were further cloned by limiting dilution. Briefly, cells were seeded into 96-well culture plates at a density of 0.5 cells/well in DMEM supplemented with 10% FBS and 20% conditioned medium obtained from supernatants of BHK-21 cell cultures. The development of foci corresponding to unique clones of cells was monitored daily and monoclonal cell lines were subcultured in DMEM supplemented with 10% FBS and 7 μg/ml blasticidin S. Transgenesis was confirmed in established cell lines by PCR.

2.4. RNA isolation

Total RNA was isolated from monolayers of transfected or infected cells using Trizol® reagent (Invitrogen, Carlsbad, USA) according to manufacturer's instructions. Similarly, total RNA was isolated from pooled supernatants of infected BHK-21 cells using Trizol® LS reagent (Invitrogen, Carlsbad, USA).

2.5. Real-time PCR

2.5.1. Reverse transcription (RT)

Except for experiments involving viral RNA, total RNA was treated with DNAse I (Invitrogen, Carlsbad, USA) prior to RT. First-strand cDNA was synthesized either using Superscript III

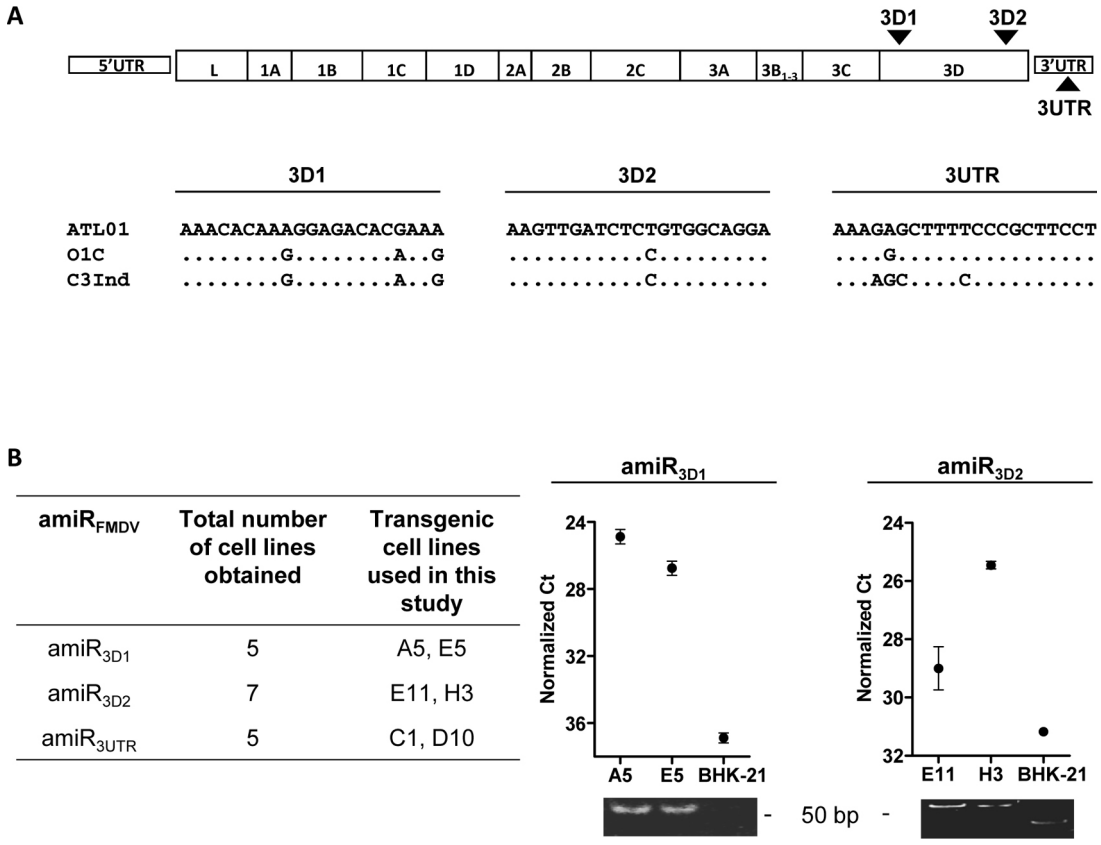

Fig. 1. Establishment of transgenic amiR$_{FMDV}$ cell lines. (A) *Top* Schematic representation of the FMDV genome showing the selected amiR target sites (black arrowheads). *Bottom* Sequence alignment showing the sequence homology between FMDV serotypes A (A/Arg/01, ATL01), O (O1 Campos, O1C) and C (C3 Indaial, C3Ind) in each target region. (B) Monoclonal cell lines obtained after stable transfection of pre-amiR$_{FMDV}$-encoding plasmids into BHK-21 cells are listed in the table. The plots show mature amiR expression as determined by stem-loop qPCR in at least two independent experiments performed in duplicate. Quantification of GAPDH mRNA was used for normalization purposes. Parental BHK-21 cells were used as negative control. Error bars represent SEM. Amplification products were revealed by 17% PAGE and ethidium bromide staining to differentiate the amplification product from stem-loop primers.

(Invitrogen, Carlsbad, USA) and stem-loop specific primers (for the detection of mature amiRs in transgenic cell lines, Table 1) or M-MLV (Promega, Madison, USA) and random hexamers (for GAPDH and reporter mRNAs and viral RNA quantification).

2.5.2. Quantification of transcripts and viral genome

Expression of RLuc, FLuc and GAPDH genes was assessed by real-time PCR as described previously (Bazzini et al., 2011) using a 10-fold dilution of cDNA as template, forward and reverse primers (Table 1), SYBR®Green (Roche Applied Science, Mannheim, Germany) and ROX (Life Technologies, Carlsbad, USA) stains and *Platinum*®Taq DNA Polymerase (Life Technologies, Carlsbad, USA). RNA levels were measured by SYBR green incorporation using following thermal cycling profile: 94 °C for 5 min, followed by 40 cycles of amplification (94 °C for 15 s, 55 °C for 30 s, and 72 °C for 40 s). In co-transfection experiments, expression of RLuc was normalized to that of FLuc.

Real-time PCR to detect viral genome in samples from growth kinetics assays was carried out with primers Epi5for and Epi2rev (Table 1) and 2× SYBR® Green PCR Master Mix (Applied Biosystems, Carlsbad, USA) with a standard cycling profile to amplify a fragment of the 3D coding region.

2.5.3. Stem-loop PCR

Real-time PCR to detect mature amiRs was performed essentially as described by Chen et al. (2005). This technique includes two steps, stem-loop RT and real time PCR. In the RT reaction, the stem-loop reverse primer binds at the 3′ portion of miR molecules and is reverse transcribed with reverse transcriptase as described in Section 2.5.1. Then, the cDNA is amplified using a miR-specific forward oligonucleotide with a 5′ tail to increase its melting temperature and a universal reverse primer that binds to the miR-unrelated sequence of the stem-loop primer. Briefly, 2 μl cDNA were used as template in a 20-μl qPCR reaction containing 10 pmol forward and Universal rev primers (Table 1), SYBR®Green (Roche Applied Science, Mannheim, Germany) and ROX (Life Technologies, Carlsbad, USA) stains and *Platinum*®Taq DNA Polymerase (Life Technologies, Carlsbad, USA). The thermal amplification profile consisted in 5 min at 94 °C followed by 40 amplification cycles (15 s at 94 °C, 30 s at 55 °C or 64 °C for amiR$_{3D1}$-amiR$_{3UTR}$ and amiR$_{3D2}$, respectively, and 40 s at 72 °C). Amplicons were cloned into pCR2.1 TOPO vector (Invitrogen, Carlsbad, USA) and a 2 nt-stretch belonging to the mature amiR and not present in either primer used for amplification was detected after automated sequencing. Normalization of mature amiR expression was performed using GAPDH as reference gene.

All qPCR reactions were performed in duplicate in an ABI 7500 Real-time PCR System (Applied Biosystems, Foster City, USA). Melting curve analysis was applied to confirm specific amplification. Data analysis and primer efficiencies were obtained using LinRegPCR Software (Ruijter et al., 2009).

2.6. Luciferase reporter transfection and activity assays

Experiments were performed in triplicate in 48-well culture plates. In brief, RLuc- and FLuc-encoding plasmids (0.9 μg) were co-transfected in a 50:1 molar ratio into BHK-21 or transgenic cell lines

Table 1
Oligonucleotides used in this study.

Reaction	Name	Sequence (5′–3′)[a]
Cloning of pre-amiR3D1	3D1top	TGCTG**TTTCGTGTCTCCTTTGTGTTT**GTTTTGGCCACTGACTGACAAACACAAGAGACACGAAA
	3D1bottom	CCTGTTTCGTGTCTCTTGTGTTTGTCAGTCAGTGGCCAAAACAAACACAAAGGAGACACGAAAC
Cloning of pre-amiR3D2	3D2top	TGCTG**TCCTGCCACAGAGATCAACTT**GTTTTGGCCACTGACTGACAAGTTGATCTGTGGCAGGA
	3D2bottom	CCTGTCCTGCCACAGATCAACTTGTCAGTCAGTGGCCAAAACAAGTTGATCTCTGTGGCAGGAC
Cloning of pre-amiR3UTR	3UTRtop	TGCTG**AGGAAGCGGAGAAAGCTCTTT**GTTTTGGCCACTGACTGACAAAGAGCTCTCCGCTTCCT
	3UTRbottom	CCTGAGGAAGCGGAGAGCTCTTTGTCAGTCAGTGGCCAAAACAAAGAGCTTTCTCCGCTTCCTC
Construction of reporter vectors, RLuc	RLfor	agatatcGCCACCATGACTTCGAAAG
	RLrev	agatatcGAATTATTGTTCATTTTTGA
Construction of reporter vectors, serotype A target sequence (fill-in)	3D1Afor	aggatccTCATTTTCTCCAAACACAAAGGAGACACGA
	3D1Arev	tctcgagatctTCAGACATTTTCGTGTCTCCTTTGTG
Construction of reporter vectors, serotype O target sequence (fill-in)	3D1Ofor	aggatccTCATCTTCTCCAAACACAAGGGAGACACAA
	3D1Orev	tctcgagatctTCAGACATCTTTGTGTCTCCCTTGTG
Construction of reporter vectors, serotype A (PCR)	3D2for	aggatccATCCTCTCCTTTGCACGCCG
	3D2rev	tctcgagatctTCAAAGAGACGCCGGTACTC
Construction of reporter vectors, serotype A (fill-in)	3UTRAfor	aggatccGAGTGAAAAGCTGGAAAGAGCTTTTCCCG
	3UTRArev	tctcgagatctGAAATAGGAAGCGGGAAAAGCTCTTTCCAG
Reverse transcription	amiR3D1rev	GTCGTATCCAGTGCAGGGTCCGAGGTATTCGCACTGGATACGACAAACAC
	amiR3D2rev	GTCGTATCCAGTGCAGGGTCCGAGGTATTCGCACTGGATACGACAAGTTG
	amiR3UTRrev	GTCGTATCCAGTGCAGGGTCCGAGGTATTCGCACTGGATACGACAAAGAG
Amplification of mature amiRs	amiR3D1for	TCGCGTTTCGTGTCTCCT
	amiR3D2for	TCGCGTCCTGCCACAGAG
	amiR3UTRfor	TCGCGAGGAAGCGGAGAA
	Universal rev	GTGCAGGGTCCGAGGT
	GAPDHfor	GCCTTCCGTGTTCCTACCC
	GAPDHrev	TGCCTGCTTCACCACCTTCA
Quantification of reporter mRNAs	RLuc913for	ATCGTTCGTTGAGCGAGTT
	miRneg seq rev	CTCTAGATCAACCACTTTGT
	FLuc53for	AGAGGATGGAACCGCTGGAGA
	FLuc152rev	GTTCACCTCGATATGTGCATCTG
Amplification of viral genome	Epi5for	TTCGAGAACGGCACTGTCGG
	Epi2rev	TCGGGGTTGCAACCGACCGC
	A6760	TCACGGTGTGTTCAACC
	A6948	GCTCAATGGGGCGTTTGCCGT
In vitro hybridization	3D1A-Alexa 647	

[a] In oligonucleotides used for cloning of pre-amiRs, mature amiRs are indicated in bold. Restriction sites are underlined.

using Lipofectamine (Invitrogen, Carlsbad, USA). After 24 h, transfected monolayers were lysed in 1× Passive Lysis Buffer (Promega, Madison, USA) to assess luciferase activity. For quantification of reporter mRNAs by real-time PCR, monolayers of transfected cells were collected in 500 μl Trizol® (Invitrogen, Carlsbad, USA).

RLuc and FLuc activities were measured on cell lysates using the Dual Luciferase Reporter Assay System (Promega, Madison, USA) and a Veritas Luminometer (Turner Biosystems, Sunnyvale, USA). To account for variations in RLuc activity due to different lengths of RLuc-target mRNAs (Fig. 2A), normalized RLuc activity in transgenic cell lines was expressed as the ratio between RLuc and FLuc activities relative to the same ratio measured in parental BHK-21 cells.

2.7. Viral growth kinetics

One-step growth kinetics was performed at a multiplicity of infection (MOI) of 5 as described previously (García Núñez et al., 2010). For multiple-step growth kinetics, cells were infected with FMDV A/Arg/01 at an MOI of 0.01, and at different times post infection supernatants were removed and cells were collected in 0.5 ml of RSB-NP40 (Tris 10 mM, pH 7.4, NaCl 10 mM, $MgCl_2$ 1.5 mM, NP40 0.01%). Lastly, the isotonicity of extracts was restored by the addition of an equal volume of 2X DMEM supplemented with 25 mM Hepes pH 7.5. Intracellular virus titers were determined by the Reed and Muench method (Reed and Muench, 1938).

2.8. RT-PCR to study viral escape mutants

Total RNA was extracted from supernatants of infected cells at different times post infection and cDNAs were synthesized as described in Sections 2.4 and 2.5.1. A 214 bp fragment encompassing the 3D1 target region was amplified from cDNAs in a standard PCR reaction using primers A6760 and A6948 (Table 1) and *Pfx* DNA Polymerase (Life Technologies, Carlsbad, USA). Amplification products were cleaned up and sequenced.

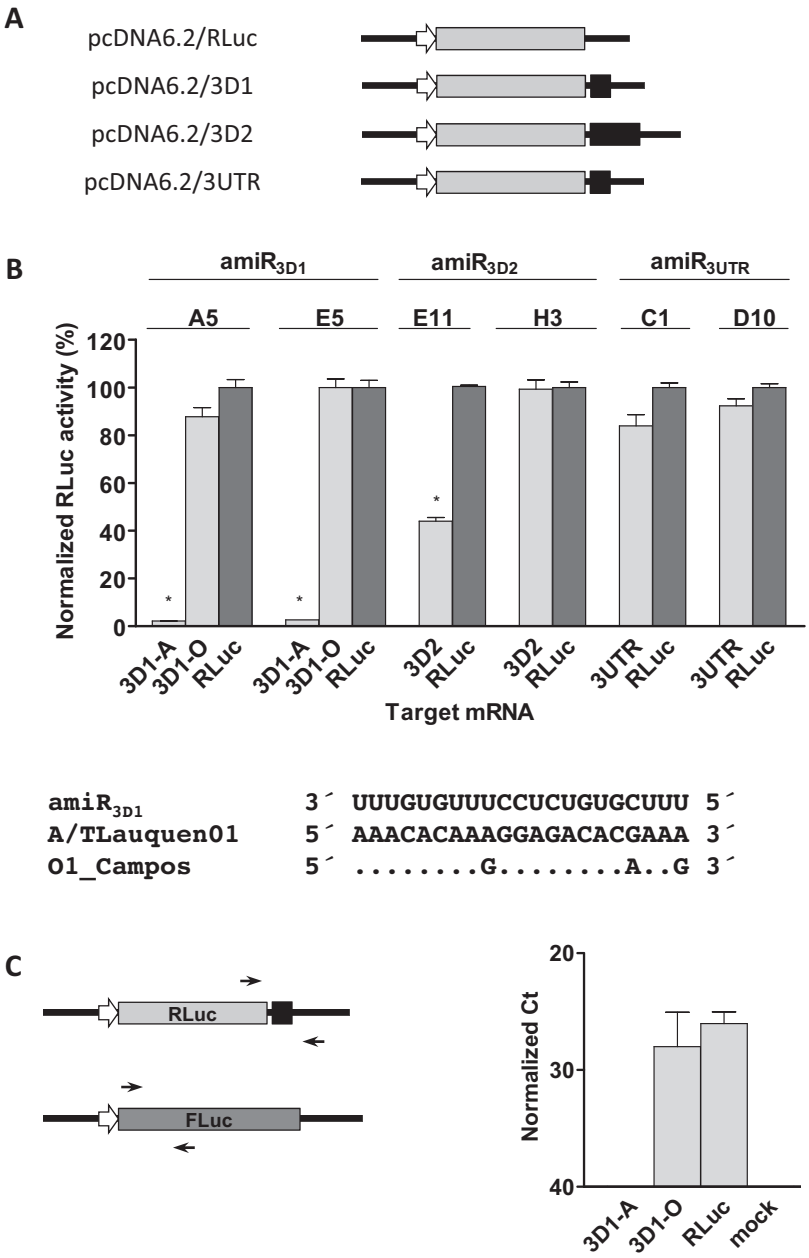

Fig. 2. Silencing activity of transgenic cell lines. (A) Schematic representation of reporter plasmids encoding RLuc (grey boxes) or RLuc fused to an FMDV fragment encompassing each amiR target sequence (black boxes). The diagrams show the different lengths displayed by RLuc reporter mRNAs. White arrows denote the CMV promoter. (B) RLuc plasmids were co-transfected with control FLuc plasmids into transgenic or parental BHK-21 cells, and *Renilla* and firefly luciferase activities were determined in cell lysates 24 h after co-transfection. Representative results of at least 3 independent experiments performed in triplicate are shown. Error bars indicate SEM. $^{*}p < 0.001$ (ANOVA or Student's *t* test). Constructs containing the 3D1 target regions from FMDV serotypes A and O (3D1-A and 3D1-O, respectively) were transfected into A5 and E5 cell lines. The sequence alignment illustrates nucleotide differences within the $amiR_{3D1}$ target sequence between both serotypes. (C) Total RNA was isolated from co-transfected $amiR_{3D1}$ cell lines and RLuc mRNA levels were quantified by real time PCR and normalized against FLuc mRNA levels (*right*). Error bars represent SEM. The diagram (*left*) shows annealing sites of primers used (black arrows).

2.9. RNA structure prediction

RNA secondary structures of amiR target sites were predicted in the context of RLuc mRNAs and the complete viral genome using MFOLD software (Zuker, 2003).

2.10. In vitro accessibility of target sequences

2.10.1. In vitro transcription

Reporter plasmids carrying the RLuc gene flanked by the T7 promoter and an FMDV target sequence were linearized by *Apa*I digestion followed by phenol:chloroform extraction and ethanol precipitation. The purified DNA was subjected to *in vitro* transcription using T7 RNA polymerase-Plus Enzyme Mix (Life Technologies, Carlsbad, USA) according to manufacturer's instructions.

For FMDV genomic RNA synthesis, a recombinant plasmid containing the full-length cDNA of strain A/Arg/01 (pA2001c, kindly provided by Dr. Soledad García Núñez) was linearized by *Not*I digestion and *in vitro* transcribed using MEGAScript T7 Kit (Life Technologies, Carlsbad, USA) following manufacturer's instructions.

Transcripts were purified by phenol:chloroform extraction followed by ethanol precipitation and resuspended in RNAse-free water. The RNA concentration was determined by measurement of

the absorbance at 260 nm and RNA integrity was verified by agarose gel electrophoresis under denaturing conditions.

2.10.2. In vitro hybridization

In vitro transcribed RNA (1 or 4 μg for RLuc or full-length FMDV molecules, respectively) was incubated in hybridization buffer (20 mM HEPES [pH 7.8], 50 mM KCl, 10 mM $MgCl_2$, 1 mM DTT) at 37 °C for 30 min in a total volume of 20 μl (native conditions) followed by addition of 10 pmol oligonucleotide 3D1A-Alexa647 (Table 1) and hybridization for 30 min at 37 °C. For hybridizations carried out under denaturing conditions, the reactions were first heat denatured at 80 °C for 15 min, chilled on ice and incubated finally at 37 °C for 30 min.

Hybridization products were subjected to 1.5% agarose gel electrophoresis in 1× TAE buffer, followed by ethidium bromide staining. Fluorescent bands corresponding to AlexaFluor 647 or ethidium bromide stained molecules were detected after excitation at 670 nm or 610 nm, respectively, in a Typhoon Trio Imager (GE Healthcare Life Sciences, Uppsala, Sweden).

2.11. RNA transfection

Viral RNA was isolated from supernatants of BHK-21 cells infected with FMDV A/Arg/01 as described in Section 2.4 and transfected into 8×10^4 cells in 96-well culture plates using DMRIE-C reagent (Life Technologies, Carlsbad, USA) following the manufacturer's instructions. Cytopathic effect (CPE) induced by viral replication was evaluated at 48 hpt by microscopic examination. The 50% tissue culture transfection dose ($TCTD_{50}$) in BHK-21 cells was calculated with the formula of Reed and Muench (Reed and Muench, 1938).

3. Results

3.1. Establishment of transgenic cell lines expressing $amiR_{FMDV}$

Three $amiR_{FMDV}$ target regions were selected within the viral genome by means of a bioinformatic prediction tool (3D1, 3D2 and 3UTR, Fig. 1A), and polyclonal cell lines stably transfected with different pre-$amiR_{FMDV}$ encoding plasmids were established. Cell lines proved positive for the transgene by PCR and, except for $amiR_{3UTR}$ cells which detached more easily from the culture surface, their phenotype looked similar to that of parental BHK-21 cells (data not shown).

Polyclonal cell lines are a mixture of cell populations that acquired the transgene in different proportions and/or have it inserted in different regions of the cellular genome. Thus, in order to avoid confusing results due to dissimilar amiR expression, polyclonal cell lines were cloned by limiting dilution and a number of monoclonal cell lines were obtained (Fig. 1B). Mature $amiR_{3D1}$ and $amiR_{3D2}$ were detected in transgenic cells by stem-loop qPCR (Fig. 1B). In contrast, the mature $amiR_{3UTR}$ was undetectable in cell lines C1 and D10 containing the pre-$amiR_{3UTR}$ transgene. This observation held true in 3 additional $amiR_{3UTR}$ cell lines obtained independently (data not shown).

3.2. Silencing activity of transgenic cell lines

Silencing activity of $amiR_{FMDV}$-expressing cells was evaluated in co-transfection experiments using the RLuc reporter gene fused to FMDV-derived sequences encompassing the corresponding $amiR_{FMDV}$ target of serotype A (Fig. 2A). As shown in Fig. 2B, normalized RLuc activity was reduced significantly in both $amiR_{3D1}$ cell lines (A5 and E5) and in one $amiR_{3D2}$ cell line (E11) although at different extents. Despite displaying a higher level of mature $amiR_{3D2}$, the remaining $amiR_{3D2}$ cell line (H3) failed to reduce RLuc activity. As expected, $amiR_{3UTR}$ cells proved no silencing activity against a reporter mRNA bearing the 3UTR target sequence.

We next evaluated whether A5 and E5 cell lines were also capable of cross-inhibiting the homologous sequence from FMDV serotype O (strain O1 Campos, Fig. 2B). Strikingly, the almost absolute silencing observed for the 3D1-A target was abolished completely when experiments were performed with the 3D1-O target exhibiting 3 nucleotide differences.

In addition, the mechanism underlying RLuc silencing was examined by qPCR amplification of the target mRNA in co-transfected A5 and E5 cells, whereby degradation of the reporter mRNA fused to the 3D1-A target was demonstrated (Fig. 2C).

3.3. Antiviral activity of $amiR_{3D1}^+$ cells

Antiviral activity of $amiR_{3D1}^+$ cells was evaluated. To this end, A5 and E5 cell lines were infected with the highly virulent A/Arg/01 strain of FMDV (MOI = 5) and intracellular viral titers and amounts of viral RNA were assessed at different times post infection. In contrast with the results obtained using the RLuc reporter, virus growth kinetics in A5 and E5 cells mimicked the one observed in BHK-21 cells (Fig. 3A), indicating that the sole expression of mature $amiR_{3D1}$ does not suffice to control viral replication. Of note, viral RNA synthesis was slightly delayed around 4 hpi in transgenic cells but this difference was not statistically significant.

Silencing of viral replication in A5 and E5 cell lines at ~4 hpi could have been overridden due to oversaturation of the silencing machinery in the experimental conditions used. So, transgenic cell lines expressing $amiR_{3D1}$ were infected at a low MOI (0.01) and intracellular viral titers were determined at different times post infection. Again, virus replication was not impaired (Fig. 3B).

Viral replication in transgenic cells could reflect FMDV adaptation to the silencing environment, e.g. by mutation of the target sequence. To test this hypothesis, the $amiR_{3D1}$ target region was amplified and sequenced from supernatants of infected cells. No mutation was detected within the amplified region (data not shown).

3.4. Accessibility of $amiR_{3D1}$ target sequence

The lack of control of viral replication in cell culture as opposed to the almost complete abrogation of reporter gene expression in A5 and E5 cell lines suggested limited recognition of the target sequence by the silencing machinery in the context of viral infection. So, different experimental approaches were used to assess accessibility of the $amiR_{3D1}$ target site both in the molecular framework of a complete viral genome and during the viral replication cycle.

The RNA secondary structure surrounding the 3D1 target site in RLuc/3D1-A and RLuc/3D1-O reporter mRNAs was predicted *in silico* and compared to the one obtained for the same region but in the context of the full-length FMDV A/Arg/01 genome. As illustrated in Fig. 4, *in silico* predictions showed the 3D1 sequence immersed within different structural environments depending on the mRNA molecule evaluated. While in the RLuc/3D1-A mRNA the FMDV target sequence was predicted to build a hairpin in which only 5 of 21 nucleotides would be involved in RNA:RNA interactions, its conformation in the context of the full-length FMDV A/Arg/01 genome appeared to be less accessible due to a higher number of RNA base pairings in the stem of the hairpin (Fig. 4B). Interestingly, in the RLuc/3D1-O mRNA the same region was theoretically comprised in a more extensively stabilized structure displaying 12 of 21 nucleotides in double-stranded RNA interactions (Fig. 4A).

To assess whether the predicted structural organization of the RNA could affect the accessibility of the 3D1 target region, hybridization reactions were carried out using *in vitro* folded target

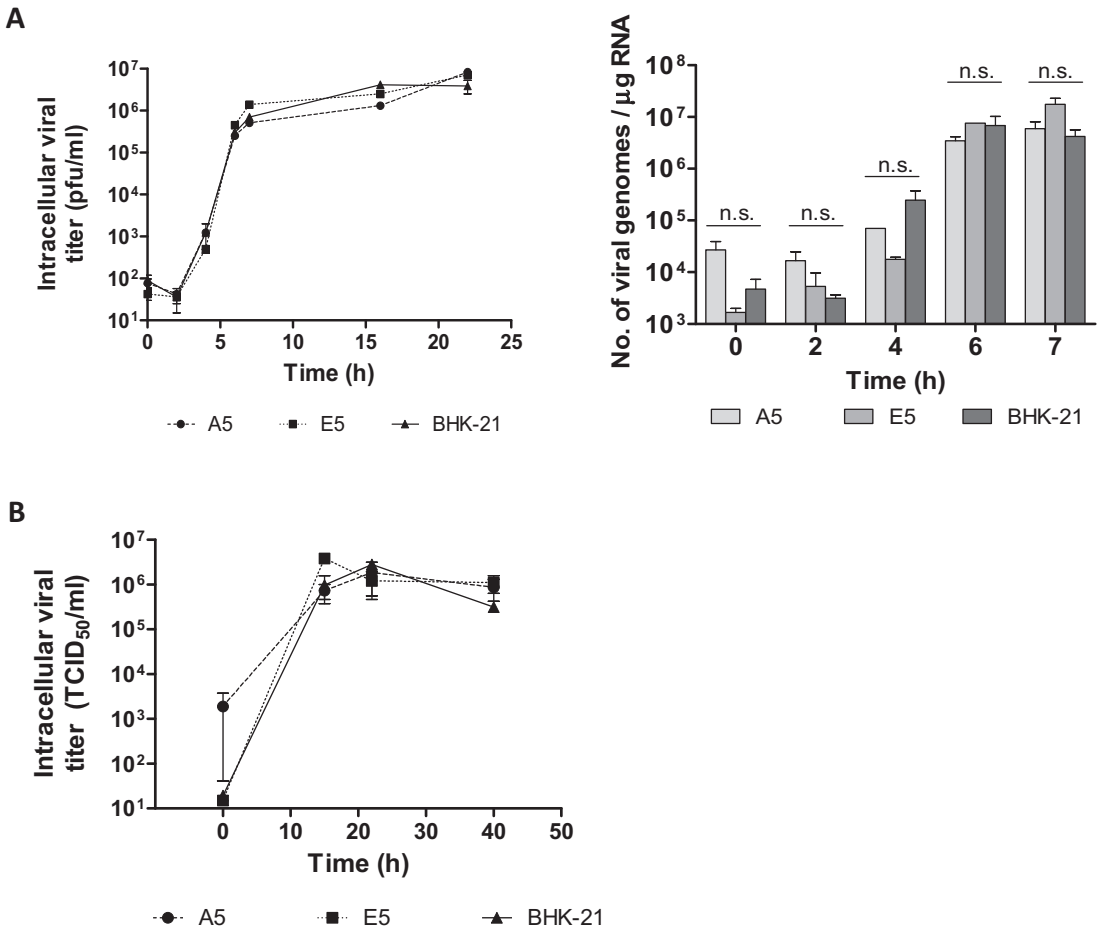

Fig. 3. Antiviral activity of amiR$_{3D1}$$^{+}$ cell lines. (A) One-step growth kinetics of FMDV strain A/Arg/01 in transgenic or parental BHK-21 cell lines, as determined by intracellular virus titration (*left*) or intracellular viral RNA quantification (*right*). Error bars represent SEM. n.s. not significant. (B) Multiple-step growth kinetics of FMDV A/Arg/01 in transgenic or parental cell lines. Error bars represent SEM.

RNA molecules and a fluorescent DNA oligonucleotide resembling the mature amiR$_{3D1}$. As shown in Fig. 4C, the amiR$_{3D1}$ target sequence was able to bind the labeled oligonucleotide under native conditions both in the context of the RLuc/3D1-A mRNA and in the full-length FMDV A/Arg/01 RNA, suggesting that this site remains accessible to hybridization in both *in vitro* folded molecules. Notably, as shown by the higher intensity of the band corresponding to the free labeled oligonucleotide and by the faint band representing the hybrid RNA:labeled oligonucleotide, the same region presented less binding ability when located in a different molecular and structural context (RLuc/3D1-O mRNA), both under native and denaturing conditions.

The accessibility of the 3D1 target sequence might also be constrained in the context of viral replication due to RNA interaction with viral or cellular proteins during the first steps of the viral cycle. To circumvent these early events and ensure accessibility of the viral RNA to RNAi complexes, full-length FMDV/A/Arg/01 RNA was isolated from supernatants of infected cells and transfected into A5 and E5 cell lines. No difference in cytopathic effect was evidenced when transgenic cells were transfected with 5 TCTD$_{50}$ as compared to parental BHK-21 cells (Fig. 5), indicating that the nude viral RNA was not subjected to amiR-mediated silencing.

4. Discussion

The antiviral strategy reported in this work was based on the constitutive expression of amiRs designed to recognize target sequences on the FMDV RNA specifically thus triggering RNAi-mediated silencing of the viral genome and controlling viral replication. Three target sequences within the viral genome were selected by means of a widely used *in silico* prediction approach, which were located within the viral RNA polymerase (3D) coding sequence and the 3′UTR of the FMDV genome. The 3D and 3′UTR regions were chosen because they are relatively conserved among different FMDV isolates as they play an essential role in virus biology. Moreover, other sequences within these genomic regions had been targeted effectively in other RNAi-mediated antiviral approaches (Du et al., 2011; Liu et al., 2005).

It is well known that transgene expression is modulated by chromatin structure and epigenetic modifications that may even lead to silencing of the exogenous gene. In this work, a number of monoclonal cell lines stably transfected with pre-amiR expressing cassettes were established and the expression and processing of these precursors were evaluated. As expected, mature amiR$_{3D1}$ was detected in A5 and E5 cell lines, which in turn proved to be functional as determined in reporter-based transfection experiments. Conversely, even though the pre-amiR was transcribed constitutively from the strong CMV promoter and processed properly in amiR$_{3D2}$$^{+}$ cells, the silencing ability of these cell lines was at most limited, revealing the unpredictability of amiR efficacy. This lack of correlation between mature amiR expression and effective gene knockdown has been reported elsewhere (Maczuga et al., 2012) and poses a challenge to the development of amiR-based silencing approaches. Regarding amiR$_{3UTR}$, the lack of detection of its mature form in five independent cell lines probably reflects some kind of constraint to the expression of this particular amiR

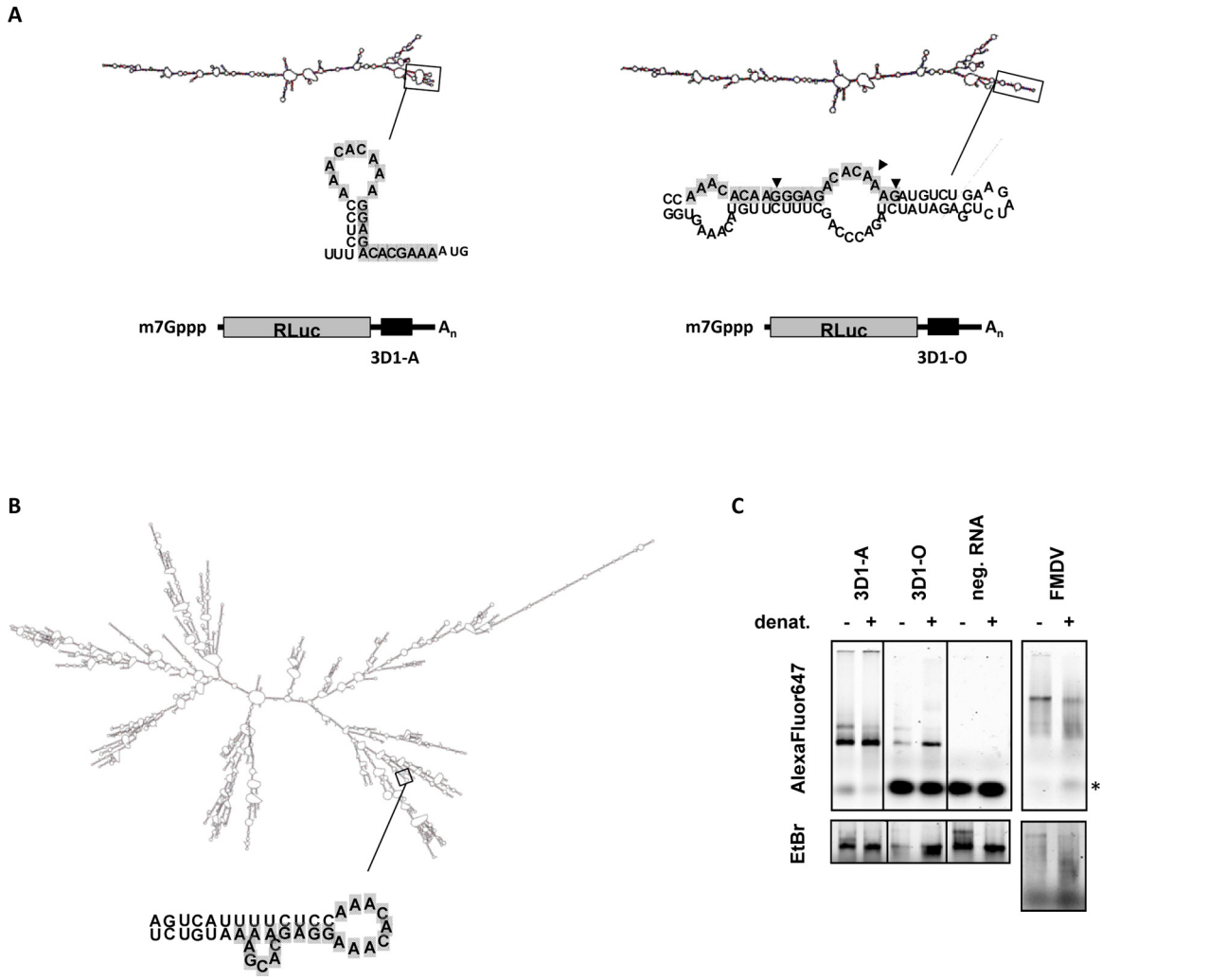

Fig. 4. *In vitro* accessibility of the 3D1 target sequence in different molecular backgrounds. Predicted secondary structure of RLuc reporter mRNAs (A) and a complete FMDV genome (B), as determined with MFOLD software ($\Delta G = -288.81$ kcal/mol, −296.18 kcal/mol and −2612.30 kcal/mol for RLuc/3D1-A mRNA, RLuc/3D1-O mRNA and FMDV RNA, respectively). The RNA conformation in the environment of the target site is magnified and nucleotides belonging to the 3D1 sequence are highlighted in grey. Arrowheads denote nucleotides within the $amiR_{3D1}$ target region that differ between FMDV serotypes A and O. **C** *In vitro* transcribed RLuc reporter mRNAs or full-length FMDV RNA were hybridized (both under native and denaturing conditions) with an AlexaFluor647-labeled oligonucleotide complementary to the 3D1 sequence and RNA:DNA hybrids were subjected to agarose gel electrophoresis to assess accessibility of the target sequence in each molecular context. Ethidium bromide staining of the gel (EtBr) was performed to visualize the amount of loaded RNA in each lane. An unrelated RNA molecule (neg. RNA) was used as negative control. The asterisk denotes migration of free labeled oligonucleotide. The image shows representative results of at least three independent experiments.

from an otherwise functional backbone for reasons not clearly understood.

In mammalian cells, endogenous miRs are partially complementary to their target mRNAs, and thus the favored gene silencing mechanism is translational repression over RNA degradation (Fabian et al., 2010). However, in order to abrogate viral replication, amiRs targeting FMDV should cleave ideally the viral RNA. Here, degradation of the reporter mRNA fused to the 3D1-A target in A5 and E5 cell lines was demonstrated by qPCR. Strikingly, the almost absolute silencing observed for the 3D1-A target was abolished completely when experiments were performed with the 3D1-O target, which demonstrates the sequence-specific nature of $amiR_{3D1}$-mediated silencing. It could be hypothesized that the nucleotide differences that exist between 3D1-A and 3D1-O sequences could account for the differences in silencing activity detected due to reduced target:amiR complementarity. In this sense, hybridization reactions carried out to evaluate *in vitro* accessibility of the 3D1-O target showed less binding ability to an oligonucleotide resembling the $amiR_{3D1}$. However, since imperfect base-pairing in the seed region (bases 2–8 of the amiR) does not

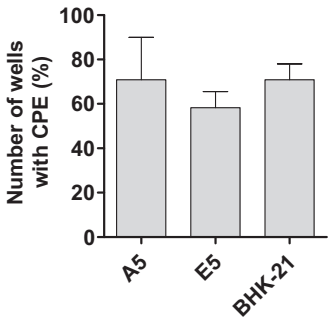

Fig. 5. Silencing activity of transgenic cell lines on nude viral RNA. Complete viral RNA was isolated from supernatants of infected monolayers and transfected into BHK-21 cells to determine the $TCTD_{50}$ as described in Section 2.11. Five $TCTD_{50}$ were transfected into transgenic or control cell lines. Bars represent mean number of wells showing CPE 48 h after transfection, as determined in three independent experiments. Error bars represent SEM.

preclude effective silencing (Brodersen and Voinnet, 2009), and given that only 1 out of 3 nucleotide differences observed between 3D1-A and 3D1-O target sequences localizes within the seed, other factors affecting the amiR$_{3D1}$-3D1-O interaction cannot be ruled out. In line with it, this target region was predicted to be constrained in a stem-loop conformation which could affect its binding to the silencing complexes present in the cytoplasm of co-transfected cells.

Antiviral activity of A5 and E5 cell lines was analyzed using the highly virulent FMDV A/Arg/01 strain (García Núñez et al., 2010), which contains the 3D1-A target sequence. Although the efficacy of amiR$_{3D1}$-mediated silencing had been demonstrated on a strong promoter-driven reporter gene, virus replication was not impaired even at a low MOI, suggesting the contribution of other factors to RNAi failure in the context of viral infection. One of these factors could be viral escape due to mutation of the target sequence, as has been reported for several plant and animal viruses (Gitlin et al., 2005; Wilson and Richardson, 2005; Simón-Mateo and García, 2006). As shown by sequence analysis of viral particles present in supernatants of infected A5 and E5 cells, the target sequence remained unchanged. However, it should be kept in mind that escape might also be accomplished by mutations outside the target region that affect its local RNA structure thus compromising its binding to the amiR (Westerhout et al., 2005).

The FMDV genome resembles an mRNA in both its orientation and the presence of a poly(A) tail at its 3′ end. Following uncoating, the viral RNA is released in the cytoplasm to initiate IRES-driven translation, a process in which the viral genome should be accessible to RNAi complexes (Grubman and Baxt, 2004). In fact, other authors observed reduced viral replication in cells expressing shRNA against FMDV (Chen et al., 2004; De los Santos et al., 2005; Kim et al., 2010; Wang et al., 2012), which places the viral genome exposed to the silencing machinery in the cytoplasm. One explanation to the lack of control of viral replication in A5 and E5 cell lines would be the existence of structural constraints imposed on the 3D1 target sequence in the context of the complete viral genome that would limit its accessibility to the amiR$_{3D1}$-charged silencing complexes. However, *in silico* prediction of the 3D1 local RNA structure and hybridization reactions using the full-length FMDV genome did not support this hypothesis, since both approaches showed results similar to the ones obtained for the 3D1 sequence in the context of the RLuc/3D1-A mRNA, which in turn was silenced successfully by these transgenic cells. Conversely, viral replication was not even controlled in transfection assays using nude viral RNA. These results suggest that the 3D1 target site is not accessible to RNAi complexes in the context of the viral genome, either with or without association to viral or cellular proteins. In conclusion, target site accessibility in the context of viral infection might limit RNAi efficacy and therefore it should be thoroughly evaluated during the development of RNAi-based antiviral approaches. Given that RNAi is mediated by large-dimension silencing complexes containing the siRNA and not simply by a linear oligonucleotide, we propose that target selection should consider not only the local RNA structure but also the global conformation of target RNA. In this sense, as demonstrated recently for HIV-1 (Low et al., 2012), high-throughput techniques like hSHAPE for the determination of the target RNA conformation appear as valuable tools for a more accurate prediction of target sites within a viral genome during the development of RNAi-mediated antiviral strategies.

Acknowledgments

This work was funded by grants from INTA (PE 232152), National Research Council (CONICET; PIP 100028 and PICT Bicentenario No. 784). M.I.G, S.A. and O.T. are members of CONICET Research Career Program.

References

Arbuthnot, P., 2011. MicroRNA-like antivirals. Biochim. Biophys. Acta 1809, 746–755.
Bazzini, A.A., Manacorda, C.A., Tohge, T., Conti, G., Rodríguez, M.C., Nunes-Nesi, A., Villanueva, S., Fernie, A.R., Carrari, F., Asurmendi, S., 2011. Metabolic and miRNA profiling of TMV infected plants reveals biphasic temporal changes. PLoS ONE 6, e28466.
Boudreau, R.L., Martins, I., Davidson, B.L., 2009. Artificial microRNAs as siRNA shuttles: improved safety as compared to shRNAs *in vitro* and *in vivo*. Mol. Ther. 17, 169–175.
Brodersen, P., Voinnet, O., 2009. Revisiting the principles of microRNA target recognition and mode of action. Nat. Rev. Mol. Cell Biol. 10, 141–148.
Carrillo, C., Tulman, E.R., Delhon, G., Lu, Z., Carreno, A., Vagnozzi, A., Kutish, G.F., Rock, D.L., 2005. Comparative genomics of foot-and-mouth disease virus. J. Virol. 79, 6487–6504.
Castanotto, D., Rossi, J.J., 2009. The promises and pitfalls of RNA-interference-based therapeutics. Nature 457, 426–433.
Chen, C., Ridzon, D.A., Broomer, A.J., Zhou, Z., Lee, D.H., Nguyen, J.T., Barbisin, M., Xu, N.L., Mahuvakar, V.R., Andersen, M.R., Lao, K.Q., Livak, K.J., Guegler, K.J., 2005. Real-time quantification of microRNAs by stem-loop RT-PCR. Nucleic Acids Res. 33, e179.
Chen, W., Yan, W., Du, Q., Fei, L., Liu, M., Ni, Z., Sheng, Z., Zheng, Z., 2004. RNA interference targeting VP1 inhibits foot-and-mouth disease virus replication in BHK-21 cells and suckling mice. J. Virol. 78, 6900–6907.
Chen, W., Liu, M., Jiao, Y., Yan, W., Wei, X., Chen, J., Fei, L., Liu, Y., Zuo, X., Yang, F., Lu, Y., Zheng, Z., 2006. Adenovirus-mediated RNA interference against foot-and-mouth disease virus infection both in vitro and in vivo. J. Virol. 80, 3559–3566.
De los Santos, T., Wu, Q., de Avila Botton, S., Grubman, M.J., 2005. Short hairpin RNA targeted to the highly conserved 2B nonstructural protein coding region inhibits replication of multiple serotypes of foot-and-mouth disease virus. Virology 335, 222–231.
Domingo, E., Escarmís, C., Baranowski, E., Ruiz-Jarabo, C.M., Carrillo, E., Núñez, J.I., Sobrino, F., 2003. Evolution of foot-and-mouth disease virus. Virus Res. 91, 47–63.
Du, J., Gao, S., Luo, J., Zhang, G., Cong, G., Shao, J., Lin, T., Cai, X., Chang, H., 2011. Effective inhibition of foot-and-mouth disease virus (FMDV) replication in vitro by vector-delivered microRNAs targeting the 3D gene. Virol. J. 8, 292.
Fabian, M.R., Sonenberg, N., Filipowicz, W., 2010. Regulation of mRNA translation and stability by microRNAs. Annu. Rev. Biochem. 79, 351–379.
García Núñez, S., König, G., Berinstein, A., Carrillo, E., 2010. Differences in the virulence of two strains of foot-and-mouth disease virus serotype A with the same spatiotemporal distribution. Virus Res. 147, 149–152.
Gitlin, L., Stone, J.K., Andino, R., 2005. Poliovirus escape from RNA interference: short interfering RNA-target recognition and implications for therapeutic approaches. J. Virol. 79, 1027–1035.
Grubman, M.J., Baxt, B., 2004. Foot-and-mouth disease. Clin. Microbiol. Rev. 17, 465–493.
Grubman, M.J., de los Santos, T., 2005. Rapid control of foot-and-mouth disease outbreaks: is RNAi a possible solution? Trends Immunol. 26, 65–68.
Israsena, N., Supavonwong, P., Ratanasetyuth, N., Khawplod, P., Hemachudha, T., 2009. Inhibition of rabies virus replication by multiple artificial microRNAs. Antiviral Res. 84, 76–83.
Kahana, R., Kuznetzova, L., Rogel, A., Shemesh, M., Hai, D., Yadin, H., Stram, Y., 2004. Inhibition of foot-and-mouth disease virus replication by small interfering RNA. J. Gen. Virol. 85, 3213–3217.
Kim, S.M., Lee, K.N., Park, J.Y., Ko, Y.J., Joo, Y.S., Kim, H.S., Park, J.H., 2008. Therapeutic application of RNA interference against foot-and-mouth disease virus in vitro and in vivo. Antiviral Res. 80, 178–184.
Kim, S.M., Lee, K.N., Lee, S.J., Ko, Y.J., Lee, H.S., Kweon, C.H., Kim, H.S., Park, J.H., 2010. Multiple shRNAs driven by U6 and CMV promoter enhaces efficiency of antiviral effects against foot-and-mouth disease virus. Antiviral Res. 87, 307–317.
Liu, M., Chen, W., Ni, Z., Yan, W., Fei, L., Jiao, Y., Zhang, J., Du, Q., Wei, X., Chen, J., Liu, Y., Zheng, Z., 2005. Cross-inhibition to heterologous foot-and-mouth disease virus infection induced by RNA interference targeting the conserved regions of viral genome. Virology 336, 51–59.
Low, J.T., Knoepfel, S.A., Watts, J.M., ter Brake, O., Berkhout, B., Weeks, K.M., 2012. SHAPE-directed discovery of potent shRNA inhibitors of HIV-1. Mol. Ther. 20, 820–828.
Maczuga, P., Koornneef, A., Borel, F., Petry, H., van Deventer, S., Ritsema, T., Konstantinova, P., 2012. Optimization and comparison of knockdown efficacy between polymerase II expressed shRNA and artificial miRNA targeting luciferase and Apolipoprotein B100. BMC Biotechnol. 12.
Pengyan, W., Jianjun, J., Ning, L., Jinliang, S., Yan, R., Chuanqfu, C., Zhiru, G., 2010. Transgenic mouse model integrating siRNA targeting the foot and mouth disease virus. Antiviral Res. 87, 265–268.
Reed, L.J., Muench, H., 1938. A simple method of estimating fifty percent endpoints. Am. J. Hyg. 27, 493–497.
Rueckert, R.R., 1996. Picornaviridae: the viruses and their replication. In: Fields, B.N., Knipe, D.M., Howley, P.H. (Eds.), Fields Virology. Lippincott-Raven, Philadelphia, pp. 609–654.

Ruijter, J.M., Ramakers, C., Hoogaars, W.M., Karlen, Y., Bakker, O., van den Hoff, M.J., Moorman, A.F., 2009. Amplification efficiency: linking baseline and bias in the analysis of quantitative PCR data. Nucleic Acids Res. 37, e45.

Simón-Mateo, C., García, J.A., 2006. MicroRNA-guided processing impairs *Plum Pox Virus* replication, but the virus readily evolves to escape this silencing mechanism. J. Virol. 80, 2429–2436.

Son, J., Uchil, P.D., Kim, Y.B., Shankar, P., Kumar, P., Lee, S.K., 2008. Effective suppression of HIV-1 by artificial bispecific miRNA targeting conserved sequences with tolerance for wobble base-pairing. Biochem. Biophys. Res. Commun. 374, 214–218.

van Rij, R.P., Andino, R., 2006. The silent treatment: RNAi as a defense against virus infection in mammals. TRENDS Biotechnol. 24, 186–193.

Wang, H., Wu, J., Liu, X., He, H., Ding, F., Yang, H., Cheng, L., Liu, W., Zhong, J., Dai, Y., Li, G., He, C., Yu, L., Li, J., 2012. Identification of short hairpin RNA targeting foot-and-mouth disease virus with transgenic bovine fetal epithelium cells. PLoS ONE 7, e42356.

Westerhout, E.M., Ooms, M., Vink, M., A.T., D., Berkhout, B., 2005. HIV-1 can escape from RNA interference by evolving an alternative sructure in its RNA genome. Nucleic Acids Res. 33, 796–804.

Wilson, J.A., Richardson, C.D., 2005. Hepatitis C virus replicons escape RNA interference induced by a short interfering RNA directed agains the NS5b coding region. J. Virol. 79, 7050–7058.

Zuker, M., 2003. Mfold web server for nucleic acid folding and hybridization prediction. Nucleic Acids Res. 31, 3406–4341.